

Atmospheric oxygen as a tracer for fossil fuel carbon dioxide: a sensitivity study in the UK

Hannah Chawner ¹, Karina E. Adcock ², Eric Saboya ^{1,7}, Tim Arnold ^{3,4}, Yuri Artioli ⁵, Caroline Dylag ³, Grant L. Forster ^{2,6}, Anita Ganesan ⁷, Heather Graven ⁸, Gennadi Lessin ⁵, Peter Levy ⁹, Ingrid T. Lujikx ¹⁰, Alistair Manning ¹¹, Penelope A. Pickers ², Chris Rennick ³, Christian Rödenbeck ¹², and Matthew Rigby ¹

¹School of Chemistry, University of Bristol, Bristol, UK

²Centre for Ocean and Atmospheric Sciences, School of Environmental Sciences, University of East Anglia, Norwich, UK

³National Physical Laboratory, Teddington, UK

⁴School of Geosciences, University of Edinburgh, Edinburgh, UK

⁵Plymouth Marine Laboratory, Plymouth, UK

⁶National Centre for Atmospheric Sciences, University of East Anglia, UK

⁷School of Geographical Sciences, University of Bristol, Bristol, UK

⁸Department of Physics, Imperial College London, London, UK

⁹Centre for Ecology and Hydrology, Edinburgh, UK

¹⁰Meteorology and Air Quality, Wageningen University and Research, Wageningen, the Netherlands

¹¹Hadley Centre, Met Office, Exeter, UK

¹²Max Planck Institute for Biogeochemistry, Germany

Correspondence: Hannah Chawner (hannah.chawner@bristol.ac.uk), Matt Rigby (matt.rigby@bristol.ac.uk)

Abstract. We investigate the use of [atmospheric](#) oxygen (O₂) and carbon dioxide (CO₂) measurements for the estimation of the fossil fuel component of atmospheric CO₂ in the UK. Atmospheric potential oxygen (APO) – a tracer that combines O₂ and CO₂, minimising the influence of terrestrial biosphere fluxes – is simulated at three sites in the UK, two of which make atmospheric APO measurements. We present a set of model experiments that estimate the sensitivity of APO simulations to

5 key inputs: fluxes from the ocean, fossil fuel flux magnitude and distribution, the APO baseline, and the [exchange](#) ratio of O₂ to CO₂ fluxes from fossil fuel combustion and the terrestrial biosphere. To estimate the influence of uncertainties in ocean fluxes, we compared three ocean O₂ flux estimates, from the NEMO – ERSEM and ECCO-Darwin ocean models, and the Jena CarboScope APO inversion. The sensitivity of APO to fossil fuel emission magnitudes and to terrestrial biosphere and fossil fuel exchange ratios was investigated through Monte Carlo sampling within literature uncertainty ranges, and by comparing

10 different inventory estimates. [We focus our model-data analysis on the year 2015 as ocean fluxes are not available for later years. As APO measurements are only available for one UK site at this time, our analysis focuses on the Weybourne station. Model-data comparisons for two additional UK sites \(Heathfield and Ridge Hill\) in 2021, using ocean flux climatologies, are presented in the Supplement.](#) Of the factors that could potentially compromise [simulated](#) APO-derived fossil fuel CO₂ estimates, we find that the ocean O₂ flux estimate has the largest overall influence at the three sites in the UK. At times, this

15 influence is comparable [in magnitude](#) to the contribution ~~to APO~~ of simulated fossil fuel CO₂ [to simulated APO](#). We find that simulations using different ocean fluxes differ from each other substantially, with no single model estimate, or a simulation with

zero ocean flux, providing a significantly closer fit to the observations. Furthermore, the uncertainty in the ocean contribution to APO could lead to uncertainty in defining an appropriate regional background from the data. Our findings suggest that the contribution of non-terrestrial sources ~~need to be well accounted for~~ needs to be better accounted for in model simulations of APO in the UK, in order to reduce ~~their~~ the potential influence on inferred fossil fuel CO₂ using APO.

1 Introduction

Variations in atmospheric carbon dioxide (CO₂) concentrations are due to atmospheric transport and the influence of fluxes from the terrestrial biosphere, the ocean and human activities. With the ultimate aim of evaluating national emission estimates, a major goal of several recent studies has been the isolation of only those variations due to anthropogenic fossil fuel CO₂ emissions. Radiocarbon, ¹⁴C, (¹⁴C) has been widely used as a tracer for this purpose (e.g. ~~????~~), as (e.g. ~~????~~). As fossil fuel emissions are ~~fully depleted devoid~~ in ¹⁴C, ~~providing a signature with which to discriminate fossil fuel emissions from other sources and sinks~~ they can be distinguished from biospheric and oceanic processes. However, ~~such~~ atmospheric ¹⁴C measurements are expensive, they cannot be made continuously to the required precision, and in some regions there may be significant interference of ¹⁴C ~~emission~~ emissions from gas-cooled nuclear power stations (???). An alternative tracer is carbon monoxide (CO), which is ~~released~~ produced by incomplete combustion. ~~Measurements~~ Atmospheric measurements of CO are much less expensive than those of ¹⁴C and can be made continuously (e.g. ???). However, there is large uncertainty in both the ratio of CO to CO₂ emissions from fossil fuel combustion, and the CO flux from non-fossil fuel sources and sinks (?).

? and ? show that atmospheric oxygen (O₂) and CO₂ measurements, combined into Atmospheric Potential Oxygen (APO) (?), can be used as a novel tracer for fossil fuel derived CO₂. In their study, ? show that their APO-derived CO₂ emission changes during the COVID-19 lockdowns in the UK correspond well to the changes found from bottom-up inventories. Their method, combining observations and machine-learning techniques, shows the potential of APO as a fossil fuel CO₂ (ffCO₂) tracer. The basis of this method is that the ratio of O₂ to CO₂ fluxes from the terrestrial biosphere, which are by definition removed from the O₂ signal through the use of the APO tracer (?), is relatively ~~well constrained~~ well constrained and invariant in space and time. For the land-based sources, O₂ and CO₂ fluxes to the atmosphere from photosynthesis, respiration, and combustion are strongly anti-correlated: CO₂ is taken up through photosynthesis whilst O₂ is released, and the reverse is true for respiration and combustion.

When considering ocean fluxes, the situation is more complex, ~~as differences~~ Differences in solubility (?) and carbonate chemistry (??) mean that the O₂ and CO₂ fluxes from the ocean are largely decoupled. However, previous work has indicated that the influence of ocean fluxes on the atmospheric ratio of O₂ to CO₂ ~~is~~ are generally smaller than the influence of fossil fuel combustion on short timescales (???). ? found short-term variability in APO, O₂ and CO₂ mole fractions with ~~only a~~ very small magnitude from the ocean when taking ship measurements.

There have been a number of promising attempts to incorporate O₂ modelling as a tracer for ffCO₂. ? modelled O₂ for the autumn of ~~2015 for three~~ 2014 finding good agreement with observations at two sites in the UK and the Netherlands, ~~finding good agreement with observations~~. APO modelling was investigated to derive European ffCO₂ fluxes by several groups within

50 the CO₂ Human Emissions project (CHE, work package 4, ??). Comparing with results from Δ¹⁴CO₂ and CO modelling, they found that APO-derived ffCO₂ gave the strongest correlation to direct ffCO₂ models using STILT and TNO fluxes. The APO models were affected by oceanic fluxes at some coastal sites, although for most coastal sites the ocean influence, modelled using ocean fluxes from NEMO - PlankTOM5, was considerably smaller than that of the ffCO₂.

Two measurement sites equipped with high-frequency CO₂ and O₂ instruments have been established in the UK, one at
 55 Weybourne Atmospheric Observatory (WAO) in the East-east of England and one at Heathfield telecommunications tower (HFD) in the South-south of England. In this paper, we perform simulations of CO₂ and O₂ focusing on these locations, primarily focusing on model-data comparisons at WAO for the year 2015, with further comparisons at HFD and WAO for the year 2021 presented in the supplement along with a third site-station at Ridge Hill (RGL) .Although telecommunications tower. Although atmospheric O₂ measurements are not available from RGL, it is included to examine the modelled APO further
 60 inland. We test the sensitivity of the APO simulation to changes in a set of uncertain model input parameters, to determine whether a robust tracer of national scale fossil fuel CO₂ can be derived.

1.1 Modelling Atmospheric Potential Oxygen

As O₂ is abundant in the atmosphere, dilution by trace gases can have a non-negligible effect on its mole fraction which may erroneously be attributed to an O₂ flux. To minimise this influence, atmospheric oxygen measurements are commonly reported
 65 as a ratio with respect to the atmospheric nitrogen mole fraction as δ(O₂/N₂) (?):

$$\delta(O_2/N_2) = \frac{(O_2/N_2)_{sample} - (O_2/N_2)_{reference}}{(O_2/N_2)_{reference}} \frac{(O_2/N_2)_{sample} - (O_2/N_2)_{reference}}{(O_2/N_2)_{reference}} \times 10^6, \quad (1)$$

where $(O_2/N_2)_{sample}$ is the O₂/N₂ ratio of a sample, and $(O_2/N_2)_{reference}$ is from a reference gas cylinder. δ(O₂/N₂) is expressed in “per meg”.

We can define the tracer APO (e.g. ???) that is largely unaffected by exchanges with the terrestrial biosphere, but sensitive
 70 to fossil fuel and (and cement production) and ocean fluxes. This is a weighted combination of O₂ and CO₂ which isolates the oceanic and fossil fuel (and cement production) components:

$$APO = O_2 + \alpha_B \times (CO_2 - 350), \quad (2)$$

where APO is a mole fraction, α_B is the O₂:CO₂ exchange ratio for the land biosphere, O₂ and CO₂ are the atmospheric mole fractions of O₂ and CO₂ respectively, and 350 (μmol mol⁻¹) is an arbitrary reference.

75 Equations ?? and ?? can be combined, expressing APO in units of δAPO in per meg (?):

$$\delta APO = \delta(O_2/N_2) + \left(\frac{\alpha_B}{S_{O_2}} \frac{\alpha_B}{X_{O_2}} \right) \times (CO_2 - 350), \quad (3)$$

where S_{O_2} is the standard mole fraction of O₂ in air, equal to 0.20946 (?).

1.1.1 The regional contribution to atmospheric APO

The regional contribution of atmospheric APO can be estimated by combining the mole fraction ~~contribution~~ contributions of O₂, CO₂, and N₂. Following the derivation in [?](#), ~~the deviation of APO can be expressed~~ baseline deviations of APO, expressed in per meg, can be written as:

$$\Delta(\delta APO) = \frac{Z + (\alpha_F - \alpha_B)F + \alpha_B O}{S_{O_2}(1 - S_{O_2})} \frac{(\alpha_F - \alpha_B)F + \alpha_B O + Z}{X_{O_2}} - \frac{N}{S_{N_2}} \frac{N}{X_{N_2}}, \quad (4)$$

$$= \frac{Z + F_O - \alpha_B F + \alpha_B O}{S_{O_2}(1 - S_{O_2})} \frac{F_O - \alpha_B F + \alpha_B O + Z}{X_{O_2}} - \frac{N}{S_{N_2}} \frac{N}{X_{N_2}}, \quad (5)$$

where Z and O respectively are the O₂ and CO₂ mole fraction contributions from the ocean; F and F_O are the contributions of CO₂ and O₂ respectively from fossil fuel combustion and cement production; N is the N₂ contribution; α_F and α_B are the fossil fuel and biospheric exchange ratios; and $S_{N_2} X_{N_2}$ is the mole fraction of N₂ in dry air, given as 0.78084 ([?](#)), where this and $S_{O_2} X_{O_2}$ are used to convert from ~~units of~~ ppm ($\mu\text{mol/mol}$) to per meg. ~~A correction of $(1 - S_{O_2})$ accounts for dilution effects of O₂ ([?](#)).~~

When estimating the exchange of N₂ we need only to consider the ocean contribution as the other components are assumed to be negligible ([?](#)). We assume a constant value for α_B for the UK of -1.07 ± 0.04 ([??](#)) ([?](#); [P. A. Pickers 2021, personal communication](#)). α_F varies for different fuel types, having values of -1.17 for coal, -1.44 for oil, -1.95 for gas, and 0 for cement production ([??](#)), and can be estimated for the UK by combining fossil fuel emissions estimates and fuel usage statistics, as outlined in Section [??](#). ~~Variations~~ However, variations in α_F are not well studied or constrained, ~~however~~. Therefore we follow [?](#) in assuming an uncertainty of ± 3 per cent.

95 2 Methodology

2.1 Observations

At both the measurement sites stations, WAO and HFD, atmospheric O₂ measurements are made using ‘Oxzilla’ lead fuel cell analysers (Sable Systems International Inc.) placed in series with non-dispersive infrared (NDIR) CO₂ ‘Ultramat 6E’ analysers (Siemens Corp.). The gas handling for each system is similar to that of [?](#), [?](#) and [?](#), to ensure stable pressures and flow rates are maintained and to avoid O₂/N₂ fractionation effects. A two-stage drying system ([???](#)) reduces the dew point of the sample air to approximately -90 °C. Calibration gases, consisting of secondary standards that are stored horizontally in thermally insulated enclosures, are used to characterise analyser responses on the ~~WMO~~ World Meteorological Organization (WMO) CO₂ scale maintained by ~~NOAA~~ The National Oceanic and Atmospheric Administration (NOAA) and the Scripps Institution of Oceanography scale for O₂, by employing routines and protocols similar to those of [?](#).

105 Weybourne Atmospheric Observatory (WAO; <https://weybourne.uea.ac.uk/>) is a coastal measurement station in Norfolk, in the east of England (52°57'02"N, 1°07'19"E) which has been routinely sampling CO₂ and O₂ since May 2010. Established in 1992, WAO is a Global Atmospheric Watch (GAW) Regional station, an National Centre for Atmospheric Sciences (NCAS)

Atmospheric Measurement Facility (AMF), and an Integrated Carbon Observation System (ICOS) Class 2 station. Air is alternately sampled from two identical aspirated inlets at 15 magl (?).

110 Heathfield (HFD) is a tall-tower measurement site that is part of the UK Deriving Emissions linked to Climate Change (DECC) network (?) which has been sampling CO₂ and O₂ since June 2021. The site is in an agricultural area in the south of England (50°58'36.3"N, 0°13'49.728"E), around 25 km north of the English Channel. Air is alternately sampled from two identical aspirated inlets (?) at 100 magl.

Ridge Hill is also a tall-tower measurement site in the UK DECC network in Herefordshire (51°59'50.766"N, 2°32'23.64"W).
115 Although CO₂ is sampled here, O₂ is not, ~~yet we include this site~~. We include Ridge Hill in the analysis to test the model at a more inland UK site.

The repeatability of the O₂ measurements from Weybourne, which is determined from regular measurements of a target tank, typically ranges from 1.68 ± 1.09 per meg to 3.31 ± 5.46 per meg (~~Adeock et al, in prep~~)(?). This exceeds WMO repeatability goals (?) for O₂, but is nevertheless amongst the most precise globally. The repeatability is calculated using the method
120 explained in ? and is reported with ±1σ uncertainty to represent how the measurement system repeatability varies over time. During the period February to November 2015, the O₂ measurement repeatability was significantly larger (10.71 ± 10.45) than usual, caused by poor performance of the Oxzilla analyser. As described in Section ??, we model the year 2015 as it is the most recent year for which outputs exist for all of the ocean models used. This larger repeatability does not significantly affect the accuracy of the O₂ measurements, but does compromise the detection limit, meaning that smaller synoptic variations in APO
125 (<10–20 per meg) may be masked during this period by the measurement imprecision. CO₂ repeatability was not affected, and is 0.005 ± 0.023 ppm on average at Weybourne, calculated from over 8000 target tank measurements made from 2010–2021.

2.2 Modelling APO

We use a Lagrangian particle dispersion model (LPDM) to simulate APO at the three measurement sites in the south of the UK. The key components of our simulation are the LPDM “footprints”, a set of flux estimates, and boundary conditions at the
130 edge of our domain. The following sections outline how each component was produced and used in the model.

For our analysis we focus on the year 2015, chosen because time-resolved ocean model outputs are available for all ocean models considered here, described in Section ??. Weybourne measurements are available for 2015 and are compared to the simulation in Section ??. Heathfield observations are only available from June 2021, when time-resolved ocean fluxes are not available, so model outputs, derived using climatological fluxes, are compared to the observational data for this site and shown
135 in the Supplement. Simulations at Ridge Hill are shown in the Supplement.

We also model the total CO₂ and O₂ mole fraction at Weybourne to compare the correlations with those observations to the equivalent for APO.

2.2.1 The Atmospheric Model

Simulations of atmospheric transport and dispersion are carried out using the Numerical Atmospheric-dispersion Modelling Environment (NAME III, version 7.2), the UK Met Office’s LPDM (?). NAME was run in time-reversed mode, in which we
140

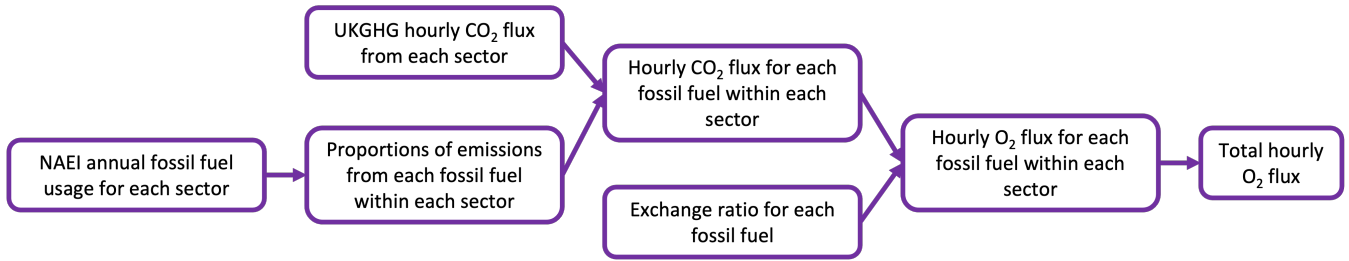


Figure 1. Calculation of UK fossil fuel O₂ fluxes from CO₂ flux estimates and fuel usage statistics from the UK National Atmospheric Emissions Inventory (NAEI), where flux estimates are downscaled to an hourly resolution using [the UKGHG \(UK Greenhouse Gas\) flux model](#).

tracked thousands of model particles back in time for 30 days from observation sites (see e.g. ?). The motion of hypothetical “particles” is simulated based on meteorological fields from the Met Office Unified Model analyses (?). The “footprint” of each measurement was estimated by recording locations and times at which particles interacted with the Earth’s surface (defined as being the lowest 40 m of the atmosphere in this case). These footprints define the sensitivity of mole fractions at a measurement site to the flux from each grid cell in the domain. Our domain covered most of Europe, the east coast of North and Central America, and North Africa, extending across the longitude/latitude range: 10.729 - 79.057°N and 97.9°W - 39.38°E (shown in Supplementary Figure S1). The footprints have the resolution 0.234° by 0.352° (roughly 25 km by 25 km over the UK).

The NAME footprints used for this study are disaggregated in time with the method described by ?. To account for the influence ~~on the mole fractions~~ of rapid variations in CO₂ flux [on the mole fractions](#), footprints are generated hourly for the 24 hours preceding a simulated data point. Time-integrated footprints are then used for the remaining 29 days of the simulation. The modelled regional contribution to the mole fraction of a species, Y_t , at a time-step, t , can then be estimated by combining the flux field with the high-time-resolution NAME footprint, as shown by equation ?? (?):

$$Y_t = \sum_{h=0}^H \sum_{j=0}^n fp_{t-h,j} \times q_{t-h,j} + \sum_{j=0}^n fp_{remainder,j} \times q_{month_j} \quad (6)$$

where H is the number of hours back in time over which the footprint is disaggregated, for which we use 24; h is the number of hours back in time before the particle release time, t ; j is the grid cell and n is the maximum number of grid cells; $fp_{t-h,j}$ is one grid cell of the footprint for that time; $q_{t-h,j}$ is one grid cell of the flux field; $fp_{remainder,j}$ is the remaining 29-day footprint; and q_{month_j} is the monthly average flux for the grid cell (by calendar month). ? discusses this method in more detail, including the effects of varying the level of time-disaggregation of the footprint, H .

2.2.2 Flux products

160 We model the regional contribution to APO separately for each of the components of Equation ?? (Z , F_O , F , O), using Equation ?? to combine the flux estimates and NAME footprints. Here we describe how the fluxes for each component are estimated.

Anthropogenic CO₂ flux estimates for the UK are taken from the UK National Atmospheric Emissions Inventory (NAEI), where estimates at a downscaled hourly resolution are derived using the UKGHG model (?)(?). Outside of the UK, anthropogenic flux estimates from EDGAR (Emissions Database for Global Atmospheric Research) are used. As NAEI includes the anthropogenic CO₂ flux estimates from both fossil fuel and non-fossil fuel sources (e.g. peat and biomass), we use the method described in Figure ?? and Equations ?? and ?? to remove emissions associated with non-fossil fuel sources, and thus estimate the fossil fuel UK CO₂ and O₂ flux:

$$CO_{2ff} = \sum_s \sum_e CO_{2s} R_{se} \quad (7)$$

170

$$O_{2ff} = \sum_s \sum_e CO_{2s} R_{se} \alpha_{fe} \quad (8)$$

where s is the SNAP sector (Selected Nomenclature for reporting of Air Pollutants, see e.g. ?), e is the fuel or source type (coal, oil, gas, non-combustion, or cement production), CO_{2s} is the CO₂ flux for the sector, R_{se} is the proportion of CO₂ emissions within the SNAP sector associated with the fuel type, and α_{fe} is the fossil fuel exchange ratio for the fuel type. We use NAEI statistics of the annual fuel usage for each SNAP sector¹ to determine R_{se} , assuming that the ratio of fuels used within each sector is constant throughout the year. When determining the fuel type associated with NAEI emissions estimates we follow the assumptions given by ?, that emissions from the non-energy use of fuels and solvent sector relate to non-combustion use of oil, and emissions from the production of non-metallic minerals relate to cement clinker production. Using the exchange ratio for each fuel, α_{fe} , we then convert from CO₂ to O₂ flux for each fuel within each sector, and take the sum to give the total hourly O₂ flux throughout the year. The O₂ flux from outside of the UK is estimated using EDGAR CO₂ fields and α_F estimates from GridFED (?).

We compare ocean CO₂ and O₂ fluxes derived from NEMO–ERSEM simulations (NE, ??), the ECCO–Darwin model (ED, ?) and the Jena CarboScope APO inversion (JC, ?), as well as a model with ocean fluxes excluded. All of the ocean fluxes have daily time resolution and raw spatial resolutions of $0.199^\circ \times 0.333^\circ$, $2.0^\circ \times 2.5^\circ$, and $0.066^\circ \times 0.110^\circ$ for ED, JC, and NE respectively, which are regridded to match the NAME spatial resolution for our analysis.

ED determines ocean-atmosphere transfer of O₂ and CO₂ by combining the CO₂ partial pressure difference across the air-sea interface with the relationship between wind speed and gas transfer, as described by ?. The Darwin Project biogeochemical model resolves the cycling of CO₂ and O₂ and its ocean ecology includes phytoplankton and zooplankton (?). JC estimates CO₂ and APO fluxes using a Bayesian atmospheric inversion and measurements from 23 CO₂ stations and up to 10 O₂ stations

¹<https://naei.beis.gov.uk/data/data-selector>

190 (including Weybourne, ???). For the JC APO inversion oceanic CO₂ fluxes are estimated from the interpolation of pCO₂ data, Air-sea fluxes of O₂ and CO₂ in NE are calculated starting from the gradient of those gases between the atmosphere and the water and using ? to estimate the gas transfer coefficient. The concentration of O₂ and CO₂ in the water are the results of dynamical processes in the ecosystem represented in the model, and in particular photosynthesis from phytoplankton and respiration of all planktonic community as well as benthic organisms. More details on the dynamics of these gases can be found
195 in ?. For all of our APO models we use a nitrogen flux field estimated from NEMO heat fluxes by Equation ??:

$$q_{ocean_N} = -\frac{dC_{eq}}{dT} \frac{\dot{Q}}{C_p} \quad (9)$$

where dC_{eq}/dT is the temperature derivative of the solubility, \dot{Q} is the ocean heat flux (positive for transfer from the ocean to the atmosphere), and C_p is the heat capacity of seawater (?). dC_{eq}/dT is estimated using:

$$\ln C = A_0 + A_1 T_S + A_2 T_S^2 + A_3 T_S^3 + S(B_0 + B_1 T_S + B_2 T_S^2) \quad (10)$$

200 with

$$T_S = \ln\left(\frac{571.3 - T}{T}\right) \quad (11)$$

where C is the gas concentration, T is the temperature (K), S is the salinity and the A and B coefficients are defined in ?. The surface heat flux is calculated by NEMO as the balance between the non-solar heat (sum of sensible, latent and long wave heat fluxes) and the incoming solar radiation (?). Both the ocean temperature and salinity are derived from the NE simulation.

205 When modelling CO₂ and O₂ mole fractions separately, we must include a terrestrial flux component. For this we use CO₂ flux estimates from the Organising Carbon and Hydrology In Dynamic Ecosystems (ORCHIDEE, ?) model. ORCHIDEE is a dynamic vegetation model which simulates the principal biospheric processes influencing the global carbon cycle, including photosynthesis, autotrophic and heterotrophic respiration. To estimate the terrestrial O₂ flux we multiply the CO₂ flux by α_B , which we assumed is equal to 1.07 ± 0.04 (see Section ??).

210 2.2.3 APO boundary conditions

With the method of ?, we model the contribution from the boundary conditions at the edge of our domain using global atmospheric fields of APO ~~mixing ratios~~ mole fractions from the JC global APO inversion (?, version apo99X_WAO_v2021). Whilst the JC APO fields include data from WAO in their derivation, any circular influence on our results should be small, because the domain boundaries are far from the UK (~1000 km) and therefore, the WAO data should not strongly influence the gradients simulated there. These boundary conditions are propagated to the measurement site by tracking the location at which NAME model particles leave the domain, thus providing a baseline estimate at the site. The baseline estimated from the boundary conditions is adjusted for consistency with the observations. To do this, we adjust the JC background for each month such that the simulated APO during periods of minimal terrestrial influence (defined as the 90 percentile of APO in a simulation with no ocean fluxes) are consistent with the observations at the same times. The original and adjusted JC backgrounds are
220 shown in Figure S2 in the Supplement.

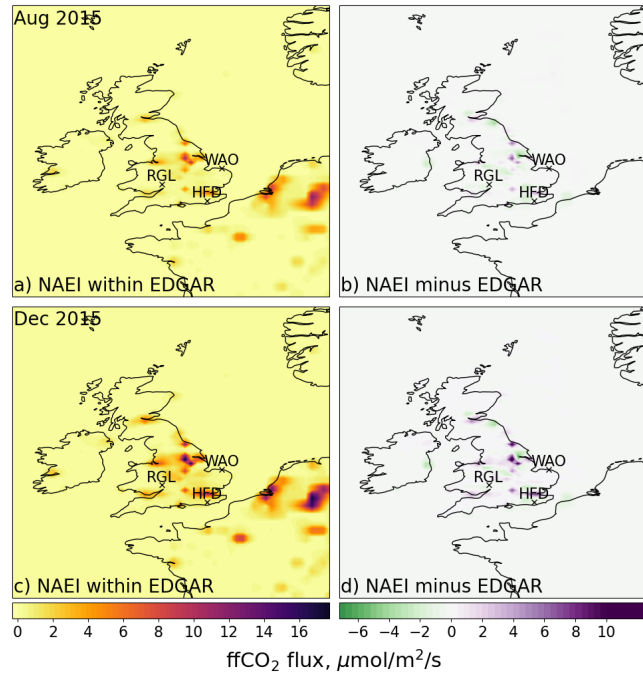


Figure 2. The ffCO_2 flux estimated by NAEI, embedded in EDGAR (panels *a* and *c*), and the difference between the NAEI and the EDGAR fields (panels *b* and *d*) for August (panels *a* and *b*) and December 2015 (panels *c* and *d*). By definition panels *b* and *d* are zero outside of the UK. The crosses show the locations of the sites included in this study: HFD, RGL, and WAO.

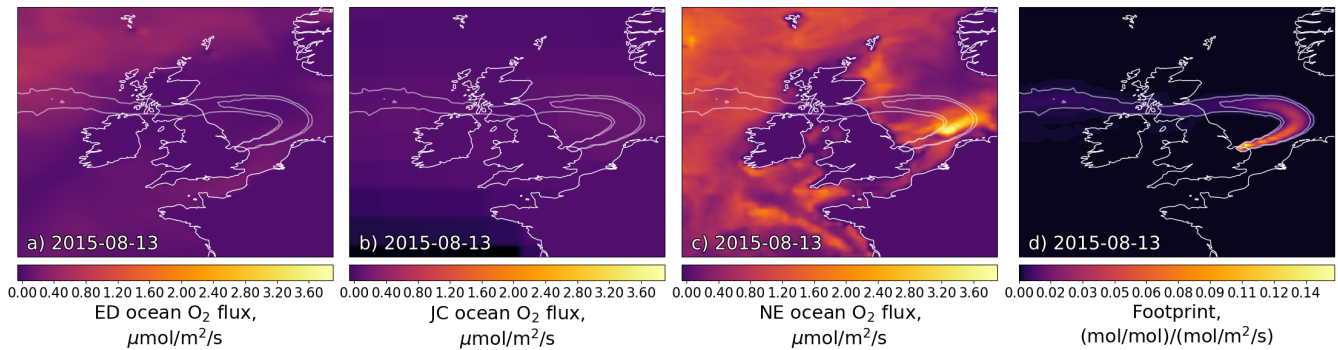


Figure 3. The daily mean O_2 ocean flux fields from the ED model (panel *a*), the JC Inversion (panel *b*) and NE model (panel *c*), and the NAME footprint (panel *d*) on the 13/08/2015 at WAO, at a time at which the ED and NE ocean fluxes dominate the simulated APO and when there is a large difference between the estimated O_2 contribution from the three flux estimates. The flux fields have the 0.002 and 0.005 $(\text{mol/mol})/(\text{mol/m}^2/\text{s})$ footprint contour overlaid.

2.3 Sensitivity experiments

Model simulations of APO are sensitive to uncertainties in several inputs of Equation ???. In this section, we outline how we investigate the sensitivities to the biospheric and anthropogenic exchange ratios (α_B and α_F), ocean fluxes, fossil fuel CO₂ emissions, baseline, and atmospheric model. [The sensitivity tests \(for APO and ffCO₂\) are summarized in Table ??](#)

Table 1. [Summary of sensitivity tests. The left-hand column indicates the parameter being investigated and whether the sensitivity to APO or ffCO₂ is being investigated. The middle column briefly describes the method employed to determine the sensitivity, and the relevant results section is shown to the right.](#)

Sensitivity test	Method	Section
APO: Biosphere exchange ratio (α_B)	Monte Carlo ensemble	3.2
APO: Fossil fuel exchange ratio (α_F)	Monte Carlo ensemble. Comparison of GridFED and NAEI-derived ratios	3.2
APO: Ocean flux estimate	Comparison of NEMO, ECCO-Darwin, Jena Carboscope flux estimates	3.3
APO: Fossil fuel flux magnitude and distribution	Monte Carlo ensemble. Comparison of NAEI and EDGAR distributions	3.4
APO: Background	Comparison of JC and REBS	3.5
ffCO₂: Ocean flux estimates	Comparison of NEMO, ECCO-Darwin, Jena Carboscope ocean fluxes	3.6
ffCO₂: Background	Comparison of JC and REBS	3.6

225 2.3.1 Sensitivity to the exchange ratios: α_B and α_F

To investigate our sensitivity to α_B and α_F in Equation ??? we employ a Monte Carlo method, randomly generating a value for each from a Gaussian distribution with a standard deviation of 0.04 mol/mol (?) and 3 per cent (?) for α_B and α_F respectively. Doing so, we generate 1000 values for the APO time-series.

As α_F varies for different fuels we must take this into account when studying the sensitivity to α_F . As described in section ??, the fossil fuel O₂ flux for each sector is calculated using α_F based on the proportion of fuels consumed within that sector. We therefore initially investigate the sector-wise sensitivity of the O₂ flux to α_F for each fossil fuel: coal, oil, and gas. Then we combine this information to determine the overall sensitivity of the fossil fuel O₂ flux and the APO simulation to α_F .

2.3.2 Sensitivity to fossil fuel flux magnitude and distribution

~~The modelled APO is dependent on fossil fuel flux estimates, and here we study~~ [We estimate](#) the sensitivity of the modelled fossil fuel contribution to the atmospheric concentration of CO₂ and O₂. ~~We first examine how the APO model may be affected by estimates of the distribution of ffCO₂ emissions. As shown in Figure ??, there are differences in the distribution of CO₂ flux estimated by two different CO₂ inventories: APO to changes in the distribution and magnitude of fossil fuel CO₂. We investigate the influence of the spatial distribution by comparing APO simulations for the NAEI and EDGAR, and we can compare the APO model using these to investigate this effect~~ [which are overall very similar in magnitude, but have a different distribution \(Figure ??\)](#). As discussed in Section ??, our APO model uses NAEI ~~ffCO₂~~ [ffCO₂](#) emissions estimates for the UK.

which are embedded in those of EDGAR ~~, as well as and combined with~~ NAEI fuel usage statistics to calculate ~~ffO₂ uptake.~~
Here we compare with EDGAR CO₂ emissions, using the GridFED estimates of ~~to estimate ffO₂ uptake.~~ We compare
these estimates to EDGAR CO₂ emissions with GridFED α_F .

We further investigate the sensitivity of the APO model to the magnitude of ~~ffCO₂ estimates~~ ffCO₂ using a Monte Carlo en-
semble in which the overall ~~CO₂ CO₂~~ flux in the entire domain is allowed to vary by $\pm 10\%$ (~~$\pm 10\%$. This range is~~ considerably
larger than the difference between EDGAR and the NAEI, which is approximately ~~0.7% 0.7%~~, but chosen so that the effect on
APO can be readily identified).

2.3.3 Sensitivity to ocean flux

Figure ?? shows the ocean flux fields from the ED and NE models and the JC inversion. For illustration, this figure is shown for
a period (13th August 2015) when the footprint for WAO is predominantly across the ocean. On this date, and in general, there
is a much larger flux in coastal regions in the NE ocean model compared with both the ED and JC estimates. Unlike exchange
ratios, the sensitivity of simulated APO to ocean fluxes cannot readily be described by an uncertainty on a single parameter.
Therefore, to examine the sensitivity to this term we produce APO timeseries using the three different flux estimates such that
we can qualitatively compare the effect on APO magnitude and variability, and compare the correlation of each model with the
observations. We also produce a timeseries with the ocean component excluded to examine whether the fit to the observations
can be improved by assuming a negligible ocean contribution.

2.3.4 Sensitivity to the background estimate

~~We study the effects of the background APO estimate on our simulations~~

~~AOs our APO simulations only account for the influence of fluxes within our regional domain, an estimate must be made~~
of the APO entering the domain. Therefore, in this section, we describe how different background estimates might influence
the comparison between the APO simulation and the observations. The background represents the APO variability that is
representative of the ~~well-mixed well-mixed~~ atmosphere at the UK's latitude, excluding local influences. ~~To do so, here we~~
We compare the modelled $\Delta(\delta\text{APO})$ (calculated using equation ??) with background-subtracted observations at Weybourne
throughout 2015. We compare two methods to subtract the background from the observations. First we estimate a baseline
from the APO observations using the 'REBS' statistical fitting routine (Robust Extraction of Baseline Signal, ??) with a span
value of 0.03, equivalent to a smoothing window of approximately one week. This smoothing window was thought to be the
most appropriate for incorporating wider-scale APO signals from outside Europe into the background term while simultane-
ously excluding local influences. For our second background subtraction we use the JC background estimate, estimated from
boundary conditions propagated to the measurement site using NAME (Section ??). A monthly adjustment is made to the
JC background to account for offsets observed in some months, as described in Section ?. This gives us two estimates of
observation-derived ffCO₂, using which we can compare the background subtraction method.

These background estimates are inherently different: for example the REBS baseline incorporates regional ocean seasonality whereas the JC estimate represents contributions from outside of the domain. However, comparing both background subtractions gives us an idea of the impact of differences between background estimates, such as their variability.

275 2.3.5 Sensitivity to the Atmospheric Model

As discussed in Section ??, in this study we use the NAME atmospheric transport model. Although NAME has been extensively inter-compared to other transport models in several publications (e.g. ???), systematic errors in NAME will influence the comparison with observations. Whilst an extensive model inter-comparison exercise is beyond the scope of this paper, to provide a simple comparison with another widely used modelling system, we compare the NAME fossil fuel CO₂ time series to that of CarbonTracker Europe (CTE2022, ??). CTE2022 uses the TM5 transport model (?) driven by ERA-5 meteorology to transport prior fluxes globally, and surface CO₂ fluxes are optimized on a weekly timestep over the period 2000–2021. The prior fluxes are from the SiB4 biosphere model (?), GFAS fire emissions (?), GridFED fossil fuel emissions (?) and JC ocean fluxes. CO₂ mole fractions based on the optimized CTE2022 at WAO are used here, with separate tracers are available for each of the described flux components.

285 2.4 Fossil fuel CO₂ mole fraction

Previous studies have indicated that we can assume that ocean fluxes do not contribute strongly to the overall APO at a measurement site over short time scales (???). Based on this assumption, it has been proposed that we can estimate regional ffCO₂ mole fractions from APO, following ?:

$$ffCO_2 = \frac{\delta APO - \delta APO_{bg}}{R_{\delta APO:CO_2}} \quad (12)$$

290 where APO_{bg} is a background APO estimate, and $R_{\delta APO:CO_2}$ is the APO:ffCO₂ ratio which can be estimated from $R_{APO:CO_2} = \alpha_f - \alpha_B$.

To estimate the time-varying ratio $R_{\delta APO:CO_2}$ in the air intercepted at the measurement site, we use the footprint-weighted fossil fuel exchange ratio:

$$R_{t,\delta APO:CO_2} = \frac{1}{\sum_{j=0}^n fp_{t,j}} \sum_{j=0}^n (\alpha_{Ft,j} - \alpha_B) fp_{t,j} \quad (13)$$

295 where t is the time, j is the grid cell and n is the maximum number of grid cells, $\alpha_{Ft,j}$ is α_F for one grid cell at that time, $fp_{t,j}$ is one grid cell of the hourly footprint at that time, and $\sum_{j=0}^n fp_{t,j}$ is the sum of the footprint across all grid cells at that time.

Here we investigate how well we can retrieve ffCO₂ mole fraction contributions from our APO models and we also estimate ffCO₂ from our observation using Equation ???. These estimates are directly compared to modeled ffCO₂ by multiplying the NAEI–within–EDGAR flux by NAME footprints, as described in Section ??. Equation ?? requires an estimate of the APO

300 background, δAPO_{bg} . When deriving $ffCO_2$ from the model we compare two methods to estimate this term: in one case by fitting a baseline to the APO model using the REBS statistical fitting routine; for comparison we use the adjusted JC background estimate. The baselines for the whole of 2015 are shown in Supplementary Figure S9. We then derive $ffCO_2$ from the below-baseline APO, comparing the effect of using of a constant value for $R_{\delta APO:CO_2}$ and that using Equation ?? to calculate a time varying exchange ratio.

305 3 Results and discussion

3.1 Simulated APO at UK measurement sites

Here we show our APO model results for 2015. As examples, one summer (August) and one winter month (December) are shown throughout, ~~and simulations~~. These months were selected based on data availability, statistical goodness-of-fit and having two months that represent sufficiently distinct parts of the APO seasonal cycle. Simulations for all months of 2015 and 310 2021 are provided in the Supplement (Figures S3 and S6).

The simulated CO_2 and O_2 mole fraction and APO contribution due to each source and sink is shown in Figure ?? for August and December 2015 at the three sites. In August, the ocean and fossil fuel mole fraction contributions have similar magnitudes and there are sustained periods during which the ocean APO component dominates over the fossil fuel. We find that there are O_2 excursions from background which are considerably larger than those inferred by ?. However, there is large disagreement 315 between the three models of ocean APO contribution, and frequently the difference between them is of a similar magnitude to that of their contribution. Whereas over the summer the ED and JC models suggest net oxygen release from the ocean, over the winter we see overall uptake due to the difference in temperature and solubility, as well as the balance of respiration and productivity. In December, the magnitude of the fossil CO_2 and O_2 mole fractions are significantly larger than that of the ocean, although there are still large differences between the ocean models. However, when converted to the fossil fuel and 320 ocean components of APO, the magnitudes are similar for Weybourne and for much of December the fossil fuel component is small compared with the ocean at Heathfield and Ridge Hill, despite these sites being further inland than WAO. For all three sites, variation between the ocean models is comparable to the magnitude of their flux and there are large periods of December during which the ocean is dominant as an O_2 sink. This is in contrast to the findings of ?, who found that the fossil fuel APO contribution was dominant at all sites, including Weybourne and Heathfield. That study used a combination of fluxes from 325 NEMO–PlankTOM5 and the atmospheric transport model STILT (?). However, ? do not provide details on the magnitude of variability in these flux estimates.

Combining the APO components using Equation ?? gives a modelled APO for Weybourne as shown in Figure ?? (for all three sites in 2015 see Supplementary Figure S3, and for Weybourne and Heathfield in 2021 see Supplementary Figure S6). Comparing with the observations we find that, although the magnitude of the variability is similar, there are substantial differ- 330 ences between the simulations and the observations. Figure ?? shows the (R^2) and root mean squared error (RMSE), comparing each ~~model set of APO simulations~~ and the observations at Weybourne for each month throughout 2015. The APO model mean of all the APO simulations for December gives a closer fit to the observations at Weybourne than the ~~model mean of all the~~

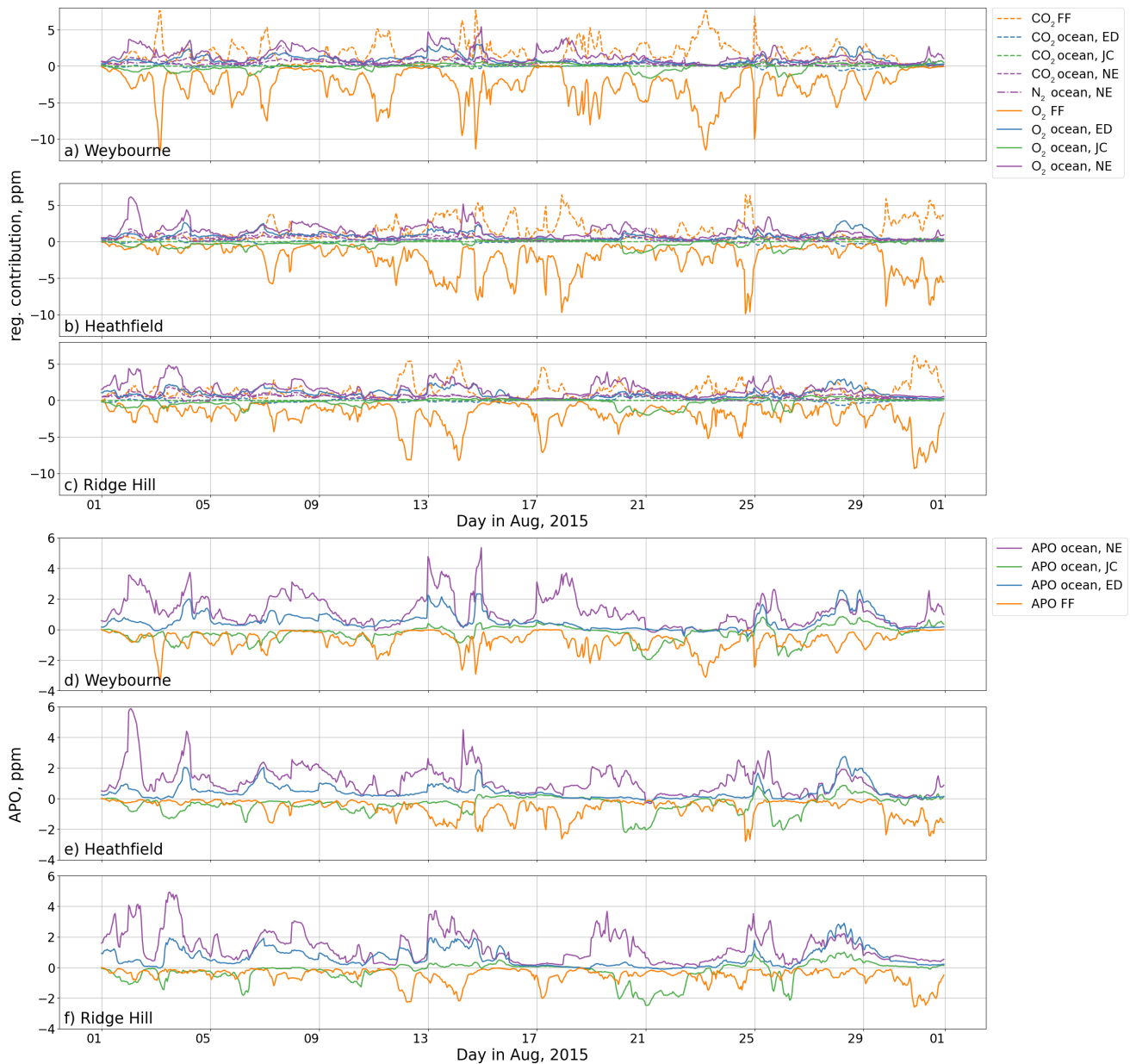


Figure 4. The regional contribution-gas-specific sectoral contributions of the ocean and fossil fuel components of APO to the mole fraction of each species at Weybourne, Heathfield, and Ridge Hill (*panels a, b, and c*) and the overall regional-APO ocean and fossil fuel contribution contributions to the APO model at the three sites (*panels d, e, and f*) throughout August 2015. The blue, green, and purple line show the contribution calculated from the ED, JC, and NE fluxes respectively, and the orange lines show the fossil fuel contributions. Solid lines represent O₂ in the top panels and APO in the bottom panels, dashed lines show the CO₂, and dash-dotted lines show the N₂.

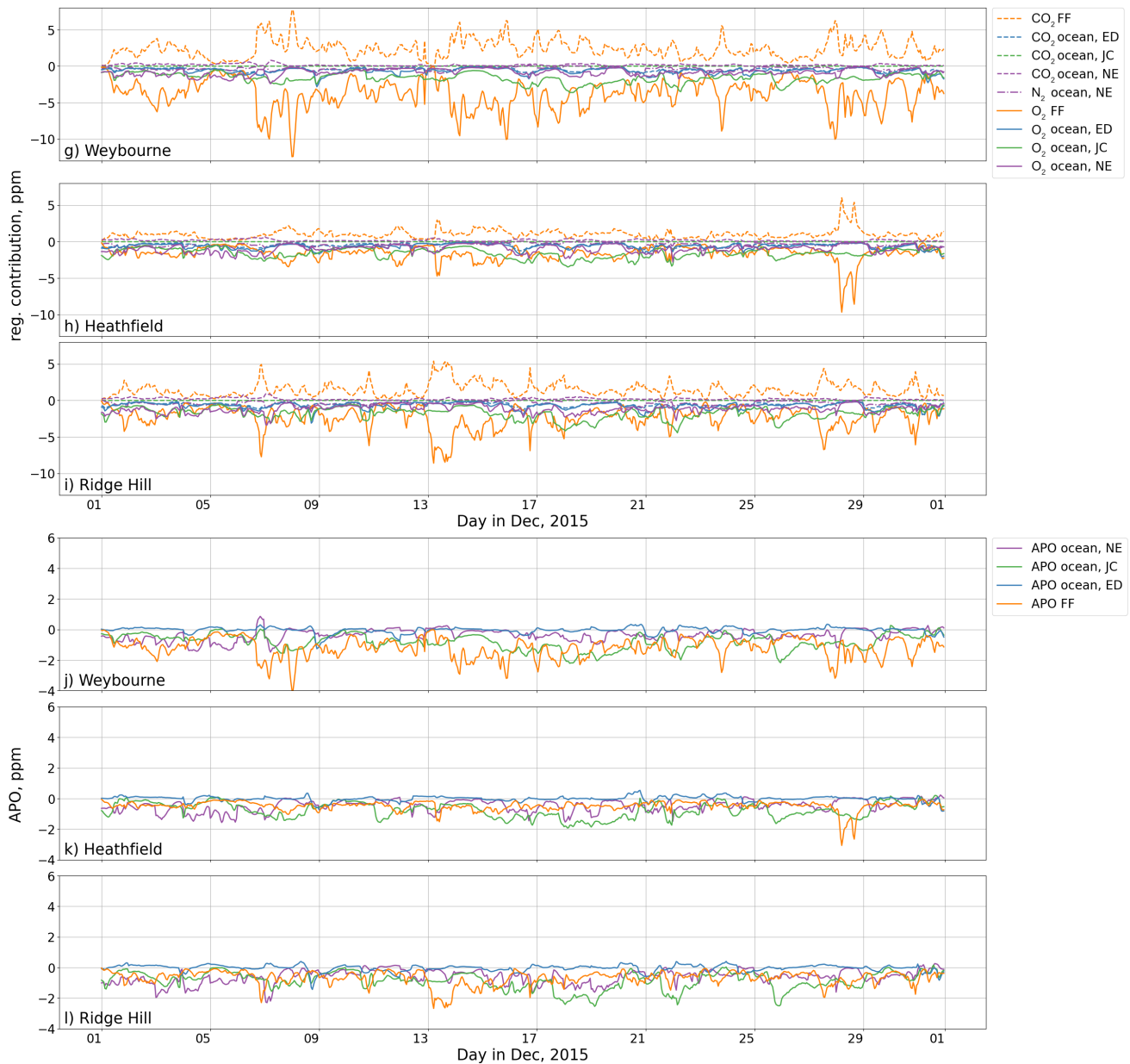


Figure 4. continued: the regional contribution of the ocean and fossil fuel components of APO to the mole fraction of each species at Weybourne, Heathfield, and Ridge Hill (*panels g, h, and i*) and the overall regional ocean and land contribution to the APO model at the three sites (*panels j, k, and l*) throughout December 2015. The blue, green, and purple line show the contribution calculated from the ED, JC, and NE fluxes respectively, and the orange line show the fossil contributions. Solid lines represent O₂ in the top panels and APO in the bottom panels, dashed lines show the CO₂, and dash-dotted lines show the N₂.

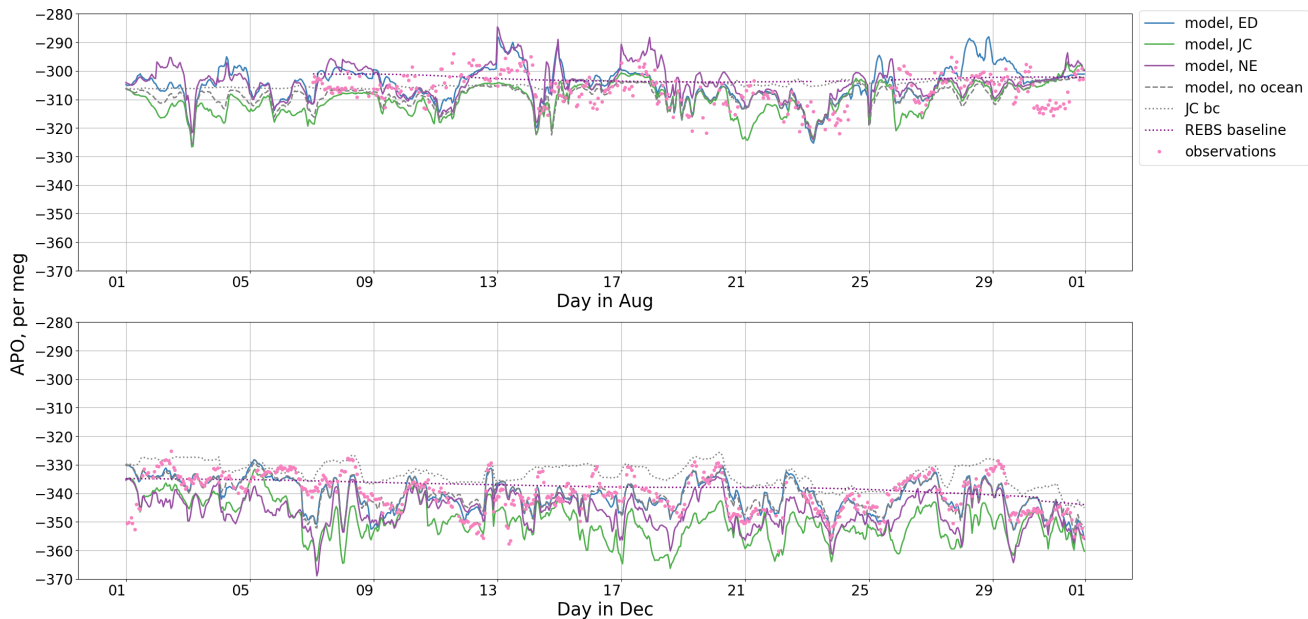


Figure 5. The modelled and observed APO at Weybourne throughout August (*panel a*) and December (*panel b*) 2015, where we model APO using three different ocean flux estimates from: the global ED ocean model (blue), the global JC inversion (green), and the regional NE ocean model (purple). We also show the APO model with no ocean contribution (grey dashed line). The dotted grey line shows the baseline derived from JC boundary conditions, which has been adjusted as described in Section ???. The magenta dots show the observations and the purple dotted line shows the baseline fit to the observations using the statistical fitting routine REBS.

[APO simulations](#) in August (average R^2 of ~~0.24~~ 0.34 vs 0.10 and average RMSE of ~~6.7~~ 9.9 ~~7.1~~ 8.4 per meg for December and August, respectively). We see a clear seasonal trend, that the correlation is lowest throughout the summer and winter and increased during the spring and autumn. This is demonstrated further in Supplementary Figure S4, where there is larger scatter over the summer months. As discussed above and shown in Figure ??, we also find that the model is more sensitive to the ocean flux over the summer, when the difference between the three APO simulations using different ocean fluxes is substantially larger (a monthly average of 7.0 per meg difference between the smallest and largest estimate in August, compared with 3.8 per meg in December). However, although our model agreement may be affected by ocean fluxes, we do not see a substantially better or worse fit when we exclude the ocean fluxes entirely, as shown in Figure ??.

The R^2 and RMSE for the CO_2 and O_2 models are shown in Figure S5 of the Supplement, where we generally see higher correlations with the data for the CO_2 and O_2 simulations (R^2 generally above 0.4) than we do for APO. We also find that our 2021 model, shown in Figure S6 in the Supplement, does not display such large variability. In that simulation, we use ocean climatologies, finding that localised ocean emission or uptake events are smoothed as they are averaged across a number of years.

Next we try filtering our model in two ways to see the effects on the correlation with the observations. First we study only daytime hours (between 11:00 and 15:00), as the boundary layer is generally more well-mixed during the day than at night and

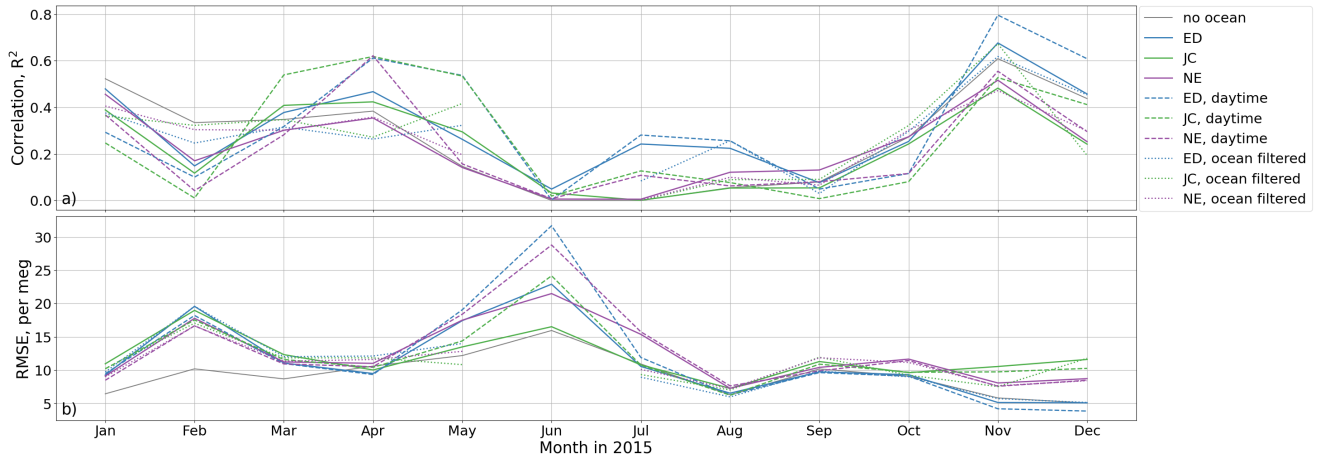


Figure 6. R^2 (panel a) and the root mean squared error (RMSE, panel b) of the modelled APO, compared with the observations at Weybourne in 2015. The blue, green, purple, and grey lines show the results from the models derived using the NAME simulations and either ED, JC, NE, and/or no ocean fluxes, respectively. The solid, dashed, and dotted lines respectively show the correlations when we do not apply any filter, and when we filter for just daytime hours, and for times when the footprint has at least 40 % sensitivity to the land.

so it is often assumed that the model-data mismatch will be smaller. Separately, we filter for times at which the footprint has at least 40 % sensitivity to the land, to investigate the effects of reducing the influence of ocean-dominated time steps. With both tests we see a small improvement in the correlation in some months, although overall, the difference with the simulations with no filtering is small (Figure ??). We further discuss the sensitivity to the ocean fluxes in Section ??.

3.2 Sensitivity to exchange ratios

The $3\text{-}\sigma$ sensitivity of APO to α_B and α_F is shown in the top and bottom panels of Figure ??, respectively ($3\text{-}\sigma$ is shown so that changes can be readily seen). In general, the model is more sensitive to α_F than α_B (average $1\text{-}\sigma$ interval of 0.27 and 0.41 per meg for α_B in August and December 2015 respectively, compared to 0.30 and 0.52 per meg for α_F). For both variables, the influence on APO of a $1\text{-}\sigma$ change is generally small compared with the difference between the observations and the model that we see in Figure ??.

We see larger sensitivity to both values of α when the mole fraction is dominated by fossil fuel fluxes. [? also identified an influence on the simulated APO due to potential misspecification of \$\alpha_B\$.](#)

3.3 Sensitivity to fossil fuel CO₂ flux

Figure ?? shows APO at Weybourne, with fossil fuel sources modelled using a combination of fluxes and exchange ratios as follows: NAEI (within EDGAR) with NAEI exchange ratios (labeled “NAEI”), EDGAR with GridFED exchange ratios (“EDGAR-GridFED”), and NAEI with GridFED exchange ratios (“NAEI-GridFED”). We find that, although there are variations in the magnitude at some time steps, the variability of the EDGAR and NAEI fossil fuel APO models is very similar. For

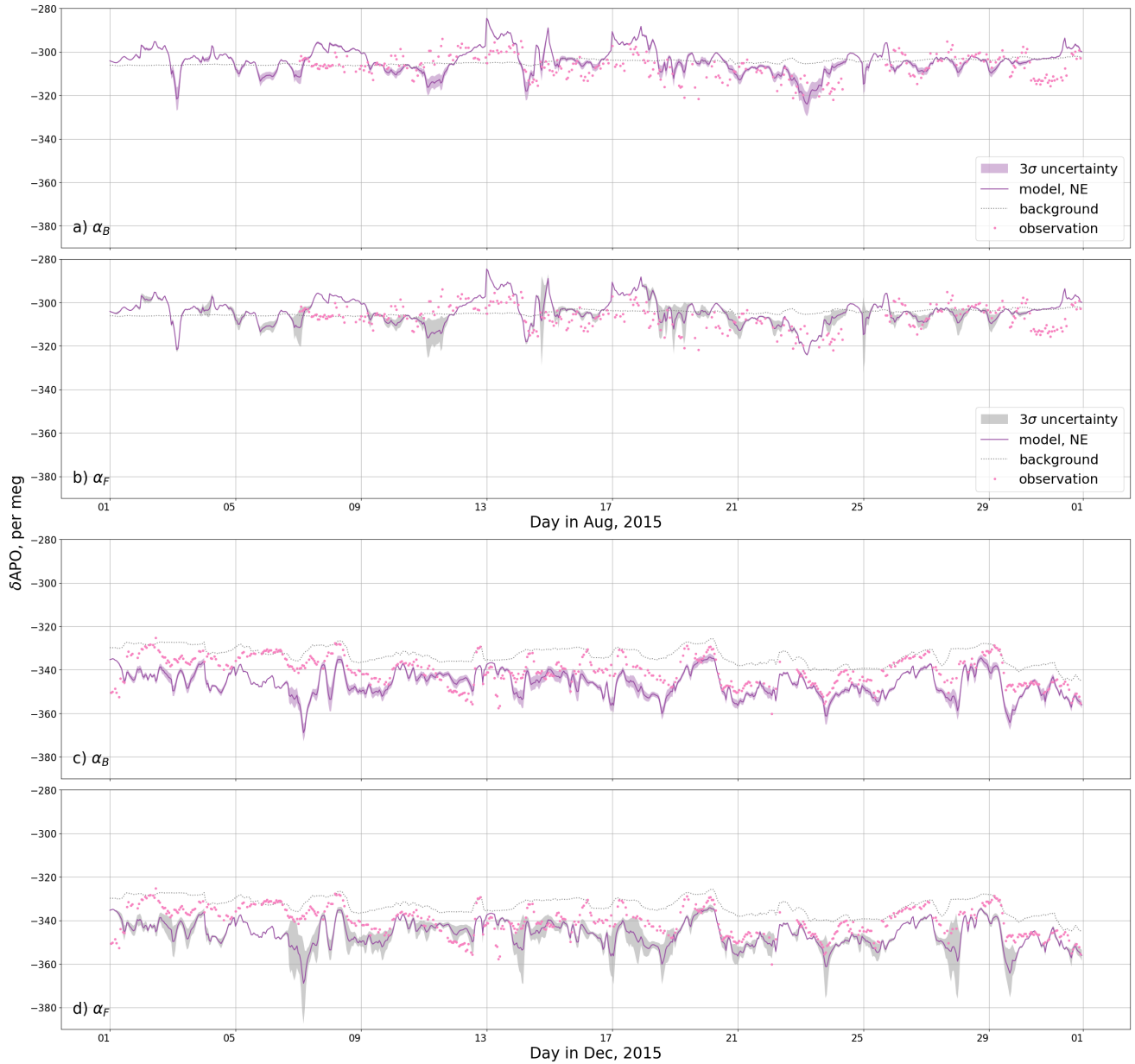


Figure 7. The APO at Weybourne during August (*panels a and b*) and December 2015 (*panels c and d*) and the sensitivity to α_B and α_F . The magenta points are the observations, the purple line is the model using NE ocean O_2 fluxes, and the shaded region is the three σ range derived from a Monte Carlo ensemble in which α_B (purple, *panels a and c*) and α_F (grey, *panels b and d*) are sampled.

Table 2. R^2 for August and December 2015, comparing the modelled APO using NAEI CO₂ fluxes and exchange ratios, EDGAR CO₂ fluxes with GridFED exchange ratios, and NAEI CO₂ fluxes with GridFED exchange ratios. For these APO models we use the NE O₂ ocean flux estimates.

	August 2015			December 2015		
	NAEI	EDGAR	NAEI-GridFED	NAEI	EDGAR	NAEI-GridFED
NAEI	~	0.957	0.999	~	0.910	0.994
EDGAR	0.957	~	0.962	0.910	~	0.911
NAEI-GridFED	0.999	0.962	~	0.994	0.911	~

R^2 for August and December 2015,

comparing the modelled APO using NAEI CO₂ fluxes and exchange ratios, EDGAR CO₂ fluxes with GridFED exchange ratios, and NAEI CO₂ fluxes with GridFED exchange ratios. For these APO models we use the NE O₂ ocean flux estimates.

the most part, the two models agree, with high R^2 in both August and December 2015, as shown in Table ???. This suggests that the choice of inventory does not have a significant impact on the simulations compared with the other components that we investigate. Additionally, in agreement with the findings of section ??, the model does not seem highly sensitive to α_F : the application of different fossil fuel exchange ratios to estimate the O₂ uptake does not cause strong disagreement between the two fossil fuel O₂ models in Figure ??, which have a high R^2 .

Figure ?? shows the modelled APO timeseries and the associated 3- σ range when sampling fossil fuel emissions magnitude with a 10% standard deviation. The sensitivity is highest when the air comes from populated areas. However, these periods of high sensitivity do not necessarily coincide with times when the discrepancy between the model and observations is highest, suggesting that errors in fossil fuel fluxes alone could not explain some of the differences between the model and observations.

3.4 Sensitivity to ocean flux

When comparing APO models and observations in Figure ?? (and Figures S3 and S4 of the Supplement), we find the biggest disagreement during the summer. At this time of year there is increased ocean productivity compared to over the winter, thus the variations between the models are larger and the APO models vary more widely. Conversely, the highest correlation between all models and the observations is seen in October (see Figure S7 of the Supplement), when the ocean acts as a small O₂ sink, and the O₂ ocean flux is smallest of any month. We see in Figures ??, ??, and Supplementary Figure S3 that the models using the ED and NE fluxes exhibit large events of O₂ release throughout the summer, which are more exaggerated in NE. At some of these times we see large differences between the ED and NE models compared with the model with no ocean component, as the ocean models indicate large APO excursions. Between April and June especially there are excursions in the NE APO model which have a much larger magnitude (up to ~85 per meg) than any in the observations. On the other hand, JC shows much smaller O₂ fluxes with generally smoother variations, and even suggests some negative APO contribution from the ocean during the summer. At some points during the summer we therefore see increased variability with NE compared with the other models. This difference may be due to the handling of coastal fluxes and the influence of rivers, which are more finely resolved in NE with its higher spatial resolution (~7km vs ~18 km), and explicit nutrient input from rivers, and by a more detailed

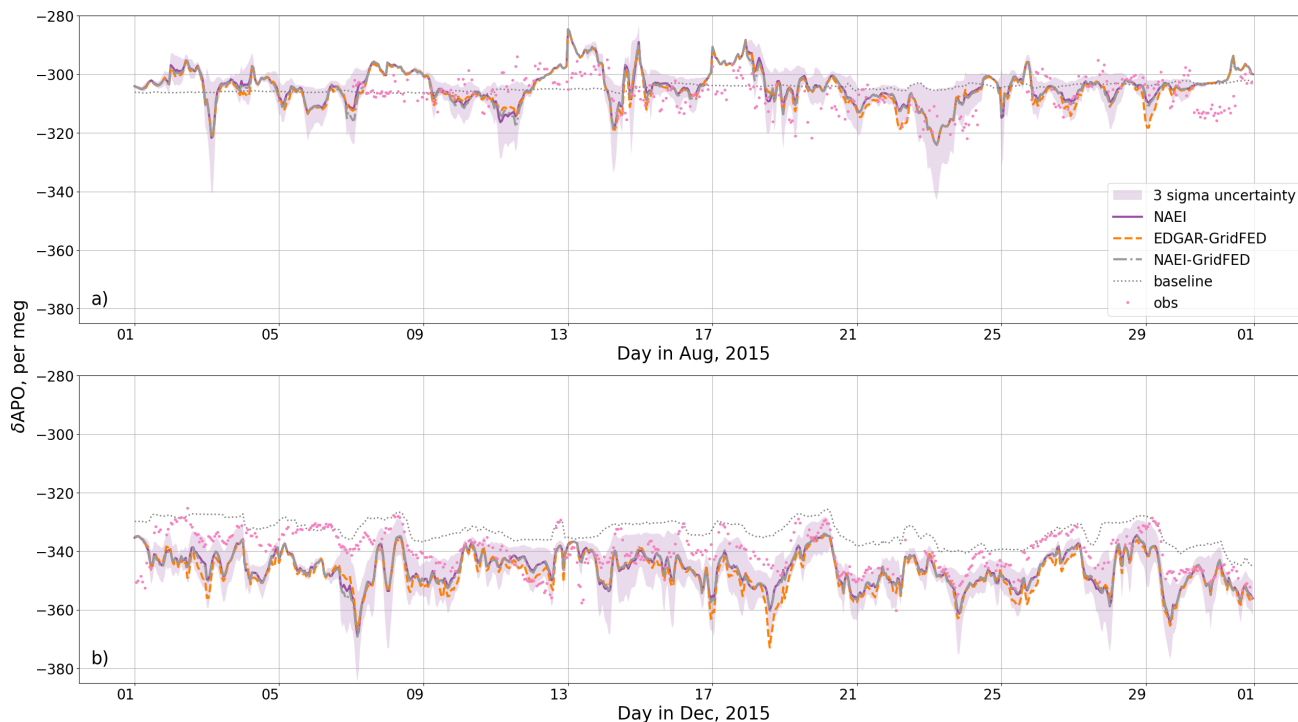


Figure 8. The APO model at Weybourne in August (*panel a*) and December (*panel b*) 2015 using NAME footprints and O₂ fluxes from the NE ocean model, comparing the model using with NAEI fluxes and exchange ratios (purple), with that using NAEI fluxes and GridFED exchange ratios (grey), and that using EDGAR fluxes and GridFED exchange ratios (orange). The observations are shown in magenta, the shaded regions represent the 3 σ uncertainty in the model assuming a 10 per cent 1 σ uncertainty on the fossil fuel component, and the grey dotted line is the background derived from JC boundary conditions.

representation of phytoplankton physiological processes (e.g. variable stoichiometry). Another factor that could contribute to the differences between the estimates of O₂ air-sea fluxes between the ocean models is the differences in the wind products used to drive the air-sea exchange and their spatial and temporal resolution.

Based on our investigation we cannot determine which, if any, of the ocean flux estimates **best** represent the APO contribution ~~to at sites in the UK on average, although there may be some events during the summer in the NE and ED simulations that are inconsistent with the data.~~ Furthermore, we do not see a substantial difference in correlation between the observations and either the simulations that include ocean fluxes or ~~that which does not~~ those that do not. ? also noted an ocean influence in their simulations using different transport models to those used here. Our result requires further investigation since the magnitude of some of the short-term ocean variability during the summer in NE and ED simulations is inconsistent with what is seen in the observations at WAO. Furthermore, it needs to be determined the extent to which these findings are due to the coastal location of WAO, since some shipboard measurements do not show a large sensitivity to ocean fluxes (?). ? suggest

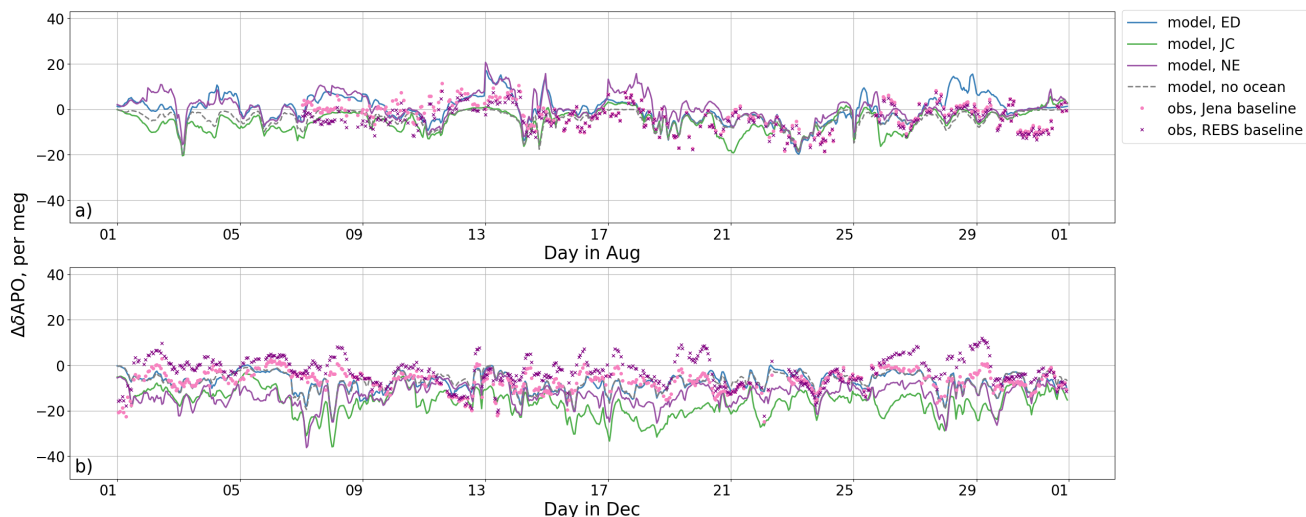


Figure 9. The modelled regional APO contribution and the background-subtracted APO observations at Weybourne throughout August (*panel a*) and December (*panel b*) 2015, where we model APO using three different ocean flux estimates from: the global ED ocean model (blue), the global JC inversion (green), and the regional NE ocean model (purple). We also show the APO model with no ocean contribution (grey line). We show two versions of background subtraction using a statistical routine (REBS, purple crosses), and using the JC background (pink points).

[that a dense continental network of stations measuring APO could minimize the potential influence of oceanic fluxes, meaning that robust estimates of fossil fuel CO₂ fluxes could be made by using observed APO gradients within a continent.](#)

3.5 Sensitivity to the background estimate

400 Figure ?? shows the modelled regional $\Delta(\delta\text{APO})$ and the background-subtracted observations. We compare the background subtraction from the statistical (REBS) filter with the adjusted model-estimated baseline from the JC global fields. For most of the time series, the two baseline estimates lead to similar regional signals. In December there is more of a difference between the two signals, where the at some regions the REBS subtracts a smaller background and leaves positive APO excursions. We expect that this difference arises because there is more variability within the JC background estimate. We saw in Figure S2 of

405 the Supplement that this variability is increased in the winter compared to summer. We see in Figure ?? that the correlation between the background-subtracted observations and the models is similar for both methods of background subtraction. Neither choice leads to a substantial difference in model-data mismatch.

3.6 Estimation of fossil fuel CO₂

Here we test how well we can retrieve the regional contribution of ffCO₂ from our modelled APO, using the method described

410 in Section ?? . Figure ?? and Supplementary Figure S10 show the comparison between ffCO₂ derived from our modelled APO

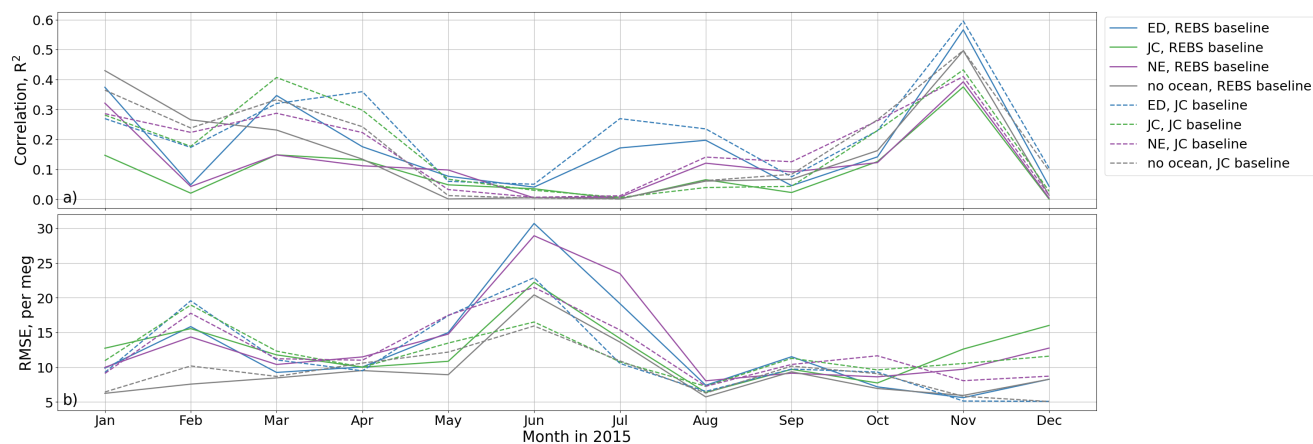


Figure 10. The square of the Pearson correlation coefficient (R^2 , *panel a*) and the RMSE (*panel b*) of the modelled regional contribution of APO, compared with the background subtracted observations at Weybourne in 2015. The blue, green, purple, and grey lines show the results from the models derived using the NAME simulations and either ED, JC, NE, or no ocean fluxes respectively. The solid and dashed lines respectively show the results when we subtract the REBS statistical background from the observations, and when we subtract the JC derived background.

and the direct simulation of ffCO_2 using NAME (i.e., ffCO_2 fluxes multiplied by NAME footprints). The comparison for all months throughout 2015 and the correlations are shown in Supplement Figure S10. Comparisons are shown when three different ocean flux estimates are used, or two different methods for subtracting the baseline. Differences between the APO-derived ffCO_2 and the direct ffCO_2 simulation will be due to the influence of ocean fluxes on the APO simulation (which is assumed negligible in Equation ??) and mis-specification of the background. All other factors, including atmospheric transport, are consistent between the two sets of simulations. Therefore, the APO-derived ffCO_2 using the adjusted JC background exactly matches the direct ffCO_2 simulation, if ocean fluxes are zero.

Firstly, we will consider the APO-derived ffCO_2 using the adjusted JC backgrounds. Throughout the summer, when there are large O_2 release events in the modelled ocean fluxes, the APO simulation using NE generally underestimates ffCO_2 , even indicating negative mole fractions for large parts of the month. The ED and JC APO simulations show closer overall agreement with ffCO_2 in August, although some discrepancy remains for all three. All three models overestimate the ffCO_2 for the majority of the winter compared to the direct ffCO_2 simulation. In this case the background APO, estimated as described in Section ??, is underestimated for large parts of the month, which may be due to modelled oceanic uptake of oxygen around the UK throughout the winter. ? found high correlations between their APO-derived ffCO_2 and direct STILT model. However, it is unclear from that work as to the time period over which this correlation was found, and it should be noted that our correlation is greatly improved when averaging over larger time periods, due to the seasonality in APO.

For the simulations in which the REBS baseline has been fit to the APO simulations and then subtracted, the derived ffCO_2 from ED and NE is higher during the summer and lower during the winter than when the adjusted JC background is used.

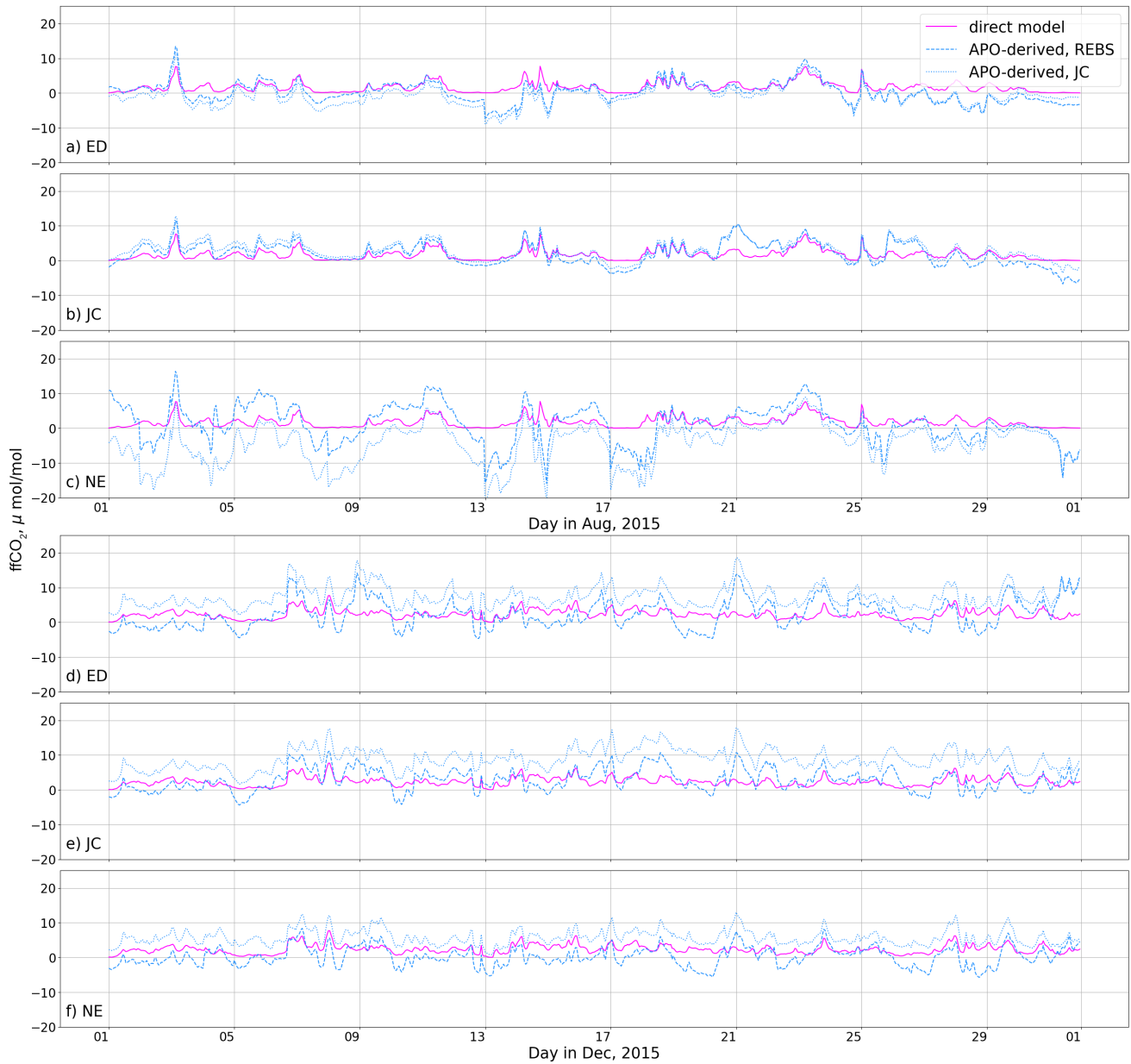


Figure 11. The modelled ffCO_2 for August (*panels a, b, and c*) and December (*panels d, e, and f*) 2015 derived from the APO model for Weybourne using the results from three different ocean flux fields (blue): ED (*panels a and d*), JC (*panels b and e*), and NE (*panels c and f*). We compare with the model calculated directly from the NAEI-within-EDGAR fluxes and NAME footprints (pink). The direct model is equivalent to the ffCO_2 in the top panels of Figure ?? and the APO models are shown in Figure ??.

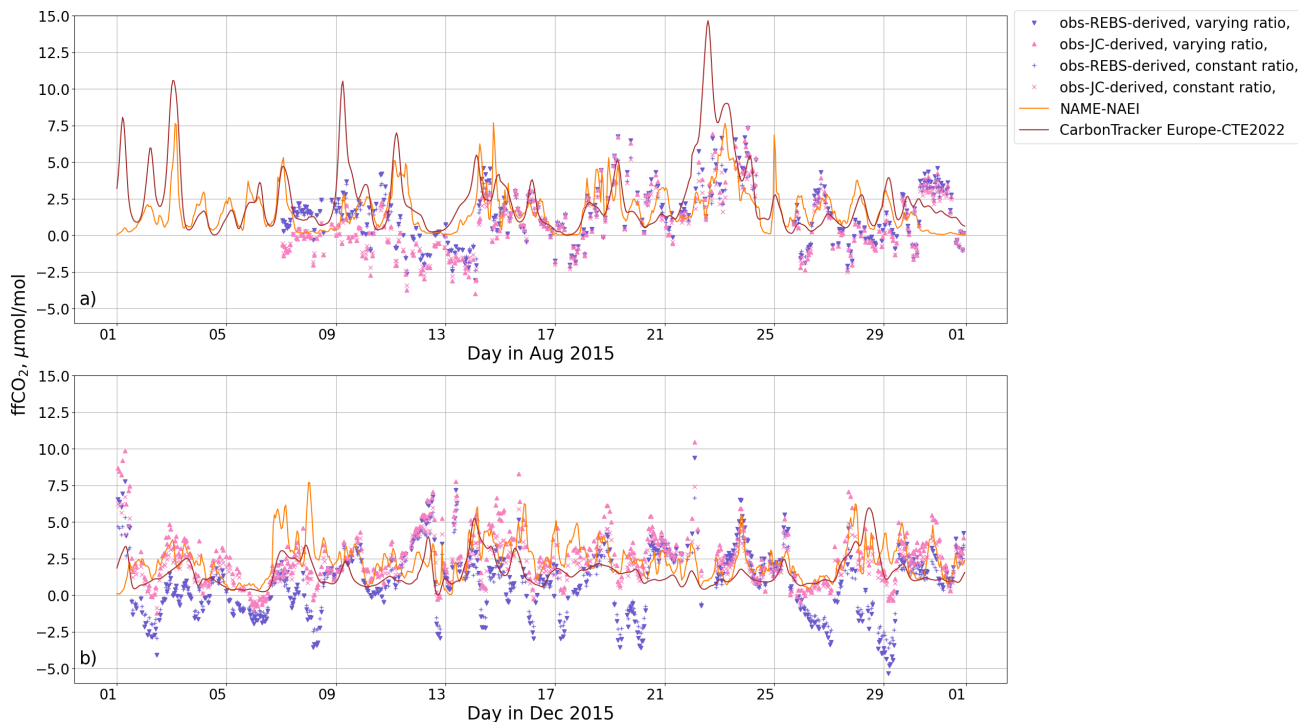


Figure 12. The regional contribution of ffCO_2 to the atmospheric abundance at Weybourne for August (*panel a*) and December (*panel b*) 2015. The pink triangles and crosses show the ffCO_2 model derived from the APO observations with the JC background subtracted using a time-varying and a constant exchange ratio respectively, the purple triangles and pluses show the same but with the REBS baseline subtracted, the orange line shows the model calculated directly from the NAEI-within-EDGAR fluxes and NAME footprints (equivalent to that in the top panels of Figure ??) and the brown line shows the model derived from CarbonTracker Europe (CTE2022).

For the model that used JC ocean fluxes, which are considerably smaller than either ED or NE, there is a much smaller
 430 difference between the two estimates. The large difference between the simulations using these two baseline estimates likely stems from the influence of ocean fluxes. The REBS fit incorporates seasonal oceanic trends and thus removes **large-timescale** long-timescale oceanic fluxes from the model. However, it is also susceptible to fitting to large APO excursions in the model which occur due to modelled short-term variability from the ocean, this is particularly clear throughout June in Figure S9 of the Supplement. On the other hand, as JC is independent of the model it does not encapsulate any regional ocean influence,
 435 and any ocean contribution is treated as ffCO_2 .

In Section ?? we make the assumption that the ocean component of the APO measurements is negligible when deriving ffCO_2 . This is based on previous studies of short-term ocean-related APO variability, which in turn are based on observations. Yet these models all indicate a persistent ocean contribution at all sites, which biases our calculation of ffCO_2 from the APO simulations. As shown in Section ??, there is large variation in O_2 flux estimates between ocean models. However, we cannot

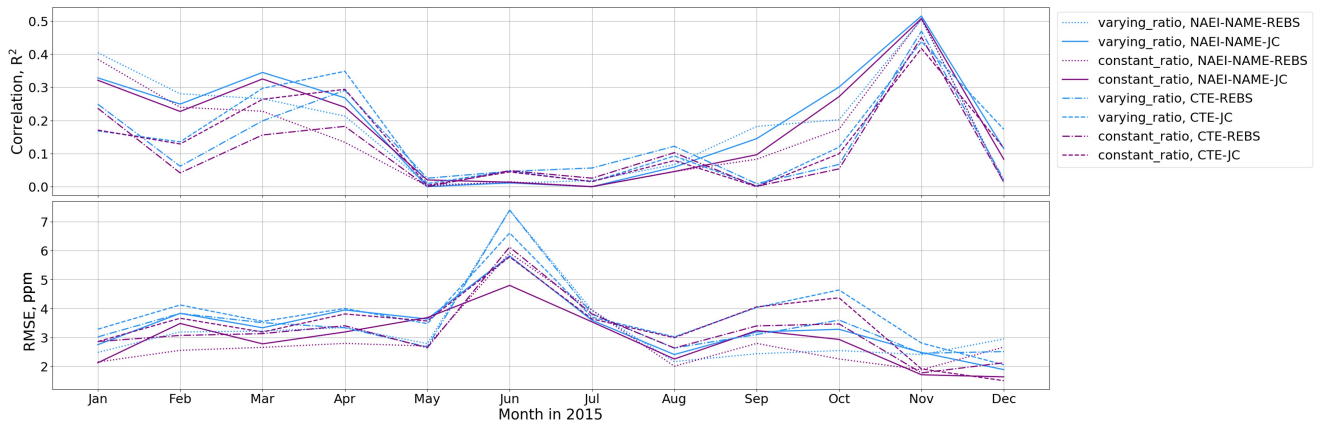


Figure 13. The ~~square of the Pearson correlation coefficient (R^2 , *panel a*) and the root mean squared error (RMSE, *panel b*) of the modelled APO, compared with the observations~~ modelled-derived and observation-derived ffCO_2 at Weybourne in 2015. The blue and purple lines show the correlation when using a time-varying and constant APO: ffCO_2 ratio respectively, the solid lines show the correlation between the NAME-NAEI model and the JC-background-subtracted observations, and the dotted lines show the same but with the REBS-background-subtracted observations. The dashed lines show the correlation between the CTE model and the JC-background-subtracted observations, and the dash-dotted lines show the same but with the REBS-background-subtracted observations.

440 conclude which model, if any, gives a more accurate representation of the ocean O_2 flux. Furthermore, the CO_2 and O_2 ocean fluxes are decoupled and therefore, the exchange ratio varies as the footprint intercepts different parts of the ocean. Based on our analysis using these three ocean flux estimates, a correction for oceanic fluxes would be subject to substantial uncertainty.

Next we apply the same method to estimate ffCO_2 from the observed APO at Weybourne (?) as described in Section ???. Figure ?? shows observation-derived ffCO_2 compared with the direct ffCO_2 simulations. Here, we have used the NAME simulation
 445 with NAEI and EDGAR fluxes, and also the outputs of the CTE system. The correlations (R^2) between the observation-derived ffCO_2 and the ffCO_2 model are shown in Figure ??. As we found in Section ??, we generally see low correlations over the summer, with stronger agreement in March, April, and November. There is not a large difference in the correlation for the JC and REBS background subtractions. This is contrary to our findings above shown in Figure ??, where we saw that there was sometimes large differences in ffCO_2 estimates for different methods of background subtraction due to the large ocean contri-
 450 bution which was assumed to be encapsulated in the background estimate. Throughout December we see that when using the REBS ~~background subtraction~~ background-subtracted observations we estimate frequent negative ffCO_2 contributions, which are not as apparent when subtracting the JC background, ~~which may~~. This could be a result of increased variability of the JC background estimate. Based on the synthetic data results presented in the previous paragraphs, discrepancies may be because of the influence of non-negligible ocean flux contributions, or errors in assigning baseline values. At ~~some~~ certain times we
 455 see a $\sim 5-8 \mu\text{mol/mol}$ difference between the direct model and the observation-derived ffCO_2 using the REBS background

subtraction; ~~this~~. This translates to an ocean contribution of $\sim 10-20$ per meg. This would be a large contribution, although the majority of the differences between the estimates are much smaller than this.

We also test the conversion of the APO observations to ffCO_2 using a constant APO: ffCO_2 ratio, assuming $\alpha_F = -1.5$, as shown by the blue points in Figure ???. Throughout the year, the correlation between this estimate of ffCO_2 and the direct model are slightly lower than when using a time-varying APO: ffCO_2 ratio. Thus we find that using a time-varying APO: ffCO_2 ratio gives a slightly closer fit to the direct ffCO_2 simulation.

4 Future outlook

~~Improvements in the measuring and modelling of tracers are important for future evaluation of ffCO_2 emissions. Our investigation has shown that there are several inputs which can sometimes substantially change the modelled APO~~ Here, we have found model-data discrepancies for APO that are relatively large compared to model-data discrepancies for O_2 and CO_2 at Weybourne in the UK. This work has used model simulations to understand the factors that could most strongly influence these differences, which can hopefully now inform further observation-based studies. In particular, a better understanding of oceanic CO_2 and O_2 fluxes in coastal regions ~~seems to be were~~ the most important of the factors ~~we tested, as such in our simulations. If a substantial oceanic influence is confirmed,~~ continental sites far from ocean influence may currently be more viable for ~~APO models. We also saw fossil fuel CO_2 estimation using APO, and/or substantially more dense APO measurement networks will be required to account for these fluxes (? , e.g.). In future, the development of alternative tracers that are sensitive to ocean fluxes and insensitive to terrestrial sources may help to better understand their relative influences. We also found~~ that the choice of baseline affects our APO model and derived ffCO_2 , although errors in assigning regional baselines may also be due in part to the influence of non-terrestrial fluxes.

Alongside APO, other tracers such as radiocarbon and CO can give extra insight into ffCO_2 emissions. Several studies have shown that radiocarbon is a promising tool for this ~~(e.g. ??)(e.g. ???)~~. However, unlike APO, most radiocarbon programs rely on flask measurements which are not continuous and require time-consuming analysis. This makes radiocarbon a comparatively expensive method which cannot presently provide such insight into high-frequency variability. Radiocarbon measurements are also susceptible to contamination of ^{14}C emissions from the nuclear power industry, correcting for which requires access to data which is not currently publicly available in the UK. Although CO ~~measurement~~ measurements are much cheaper than radiocarbon and can be made continuously (e.g. ???), the conversion from CO to ffCO_2 is uncertain.

Given the challenges of each, ~~no one tracer currently provides the answer to the verification of~~ further work is required to improve each of these tracers for ffCO_2 emissions. ~~However~~ evaluation. Here, we have identified key areas of focus which may improve the ~~modelling of APO and its use as a ffCO_2 tracer~~ use of APO for this purpose in the future.

485 5 Conclusions

We have simulated the tracer APO throughout the years 2015 and 2021 at three sites in the UK: Weybourne, Heathfield, and Ridge Hill. Generally, the correlation with the observations is ~~small for APO~~. ~~We find large~~ smaller for APO than for simulations of CO₂ and O₂. We find modelled ocean signals which sometimes dominate the APO model, and that correlations tend to be higher for APO during the spring and autumn when ocean fluxes are smallest.

490 We have presented a sensitivity analysis of the factors that most strongly influence modelled atmospheric APO. Our simulations suggest that uncertainties in ocean fluxes contribute substantially to modelled APO and APO-derived ffCO₂ ~~from the model~~ at measurement sites in the UK. Our analysis cannot determine which ocean model (or indeed, zero ocean flux) or baseline estimation method leads to closest agreement with the observations. However, a robust estimate of ffCO₂ is likely to depend strongly on these factors being ~~well known~~. ~~In comparison~~ well-known, or proven to have little influence using observation-based methods. We do not find evidence from our three UK stations that the substantial (yet uncertain) influence of oceanic fluxes on simulated APO is reduced further inland. But since the UK is surrounded by ocean, simulated APO at continental European locations may be less strongly affected. More robust ffCO₂ may be possible in general if a sufficiently dense network of sites were available, which could account for fossil fuel influences jointly with that of any oceanic sources. In comparison to the ocean fluxes and baseline, the sensitivity of ~~atmospheric~~ APO to uncertainties in fossil fuel and terrestrial biosphere exchange ratios was relatively small. Our analysis shows that further work should focus on improving ocean O₂ and CO₂ flux estimates ~~to improve the accuracy of high-frequency~~ which could improve the agreement between modelled and observation APO-derived ~~ffCO₂ in the UK~~ estimates of UK ffCO₂.

495
500

6 Code Availability

The code for the analysis presented is available at https://github.com/hanchawn/APO_modelling (?). We also use code developed by the ACRG Modelling team at the University of Bristol, which is available at <https://github.com/ACRG-Bristol/acrg>.

505

7 Data Availability

The datasets generated and analysed during this study are available at <https://zenodo.org/record/7681834> (?). The observational datasets are available on CEDA at:

- Heathfield CO₂ and O₂: <https://catalogue.ceda.ac.uk/uuid/bfc2483537a744dca8e3239278b6e522>
- 510 – Weybourne CO₂: <https://catalogue.ceda.ac.uk/uuid/87fc265aab6b4aeb961e62da2cd6ca91>
- Weybourne O₂: <https://catalogue.ceda.ac.uk/uuid/b3f9714c956f428a840211e0184e23eb>

8 Author contribution

HC carried out the atmospheric modelling and data analysis with contributions from PAP, YA, AJM, CR, GL, PL and ITL. Measurements were made by KEA and PAP, with support from TA, CD, GLF and CR. HC wrote the paper, with contributions
515 from MR, PAP, [ES](#), YA, ITL, HG, ALG and all co-authors.

9 Competing interests

The authors declare that they have no conflict of interest.

10 Acknowledgements

HC, [ES](#), MR and ALG were supported by a Natural Environment Research Council grant to the University of Bristol as part
520 of the Detection and Attribution of Regional Emissions (DARE-UK) project, NE/S004211/1. [I.T.L. received funding from Netherlands Organisation for Scientific Research \(VI.Vidi.213.143 and 2023/ENW/01426235\)](#). We thank P. Wilson, and T. Barningham for assisting with maintaining the WAO O₂ and CO₂ measurement system during 2015.

Atmospheric O₂ and CO₂ measurements at WAO in 2015 and 2021 were funded by the U.K. Natural Environment Research Council (NERC) grants NE/I013342/1, NE/S004521/1, and NE/R011532/1. The WAO atmospheric O₂ and CO₂ measurements
525 have also been supported by the U.K. National Centre for Atmospheric Science (NCAS) from 1st December 2013 onward. P.A.P., K.E.A., and G.L.F. received funding from the NERC project DARE-UK (NE/S004211/1), and P.A.P and K.E.A. have received funding from the Horizon Europe project PARIS (101081430).

YA and GL acknowledge DARE-UK (NE/S004947/1) and the U.K. National Capability NERC Climate Linked Atlantic Sector Science program (NERC grant no. NE/R015953/1).